



HAL
open science

Improved PWR LOCA simulations through refined core 3D simulations - An advanced 3D modelling and the associated METERO validation program

Dominique Bestion, Philippe Fillion, Raphaël Préa, Gilles Bernard-Michel

► To cite this version:

Dominique Bestion, Philippe Fillion, Raphaël Préa, Gilles Bernard-Michel. Improved PWR LOCA simulations through refined core 3D simulations - An advanced 3D modelling and the associated METERO validation program. NUTHOS-12 - 12th International Topical Meeting on Nuclear Reactor Thermal-Hydraulics, Operation and Safety, Oct 2018, Qingdao, China. cea-04084545

HAL Id: cea-04084545

<https://cea.hal.science/cea-04084545v1>

Submitted on 28 Apr 2023

HAL is a multi-disciplinary open access archive for the deposit and dissemination of scientific research documents, whether they are published or not. The documents may come from teaching and research institutions in France or abroad, or from public or private research centers.

L'archive ouverte pluridisciplinaire **HAL**, est destinée au dépôt et à la diffusion de documents scientifiques de niveau recherche, publiés ou non, émanant des établissements d'enseignement et de recherche français ou étrangers, des laboratoires publics ou privés.

Improved PWR LOCA Simulations Through Refined Core 3D Simulations – An Advanced 3D Modelling and the Associated METERO Validation Program

Dominique Bestion,

CEA, DEN-Service de Thermohydraulique et de Mécanique des Fluides, STMF
F-38054 Grenoble, France
dominique.bestion@cea.fr

Philippe Fillion, Raphaël Préa and Gilles Bernard-Michel,

CEA, DEN-Service de Thermohydraulique et de Mécanique des Fluides, STMF, Université Paris-
Saclay
F-91191 Gif-sur-Yvette, France
philippe.fillion@cea.fr, raphael.prea@cea.fr, gilles.bernard-michel@cea.fr

ABSTRACT

System thermalhydraulic codes have 3D models initially devoted to the prediction of large scale 3D effects during LBLOCAS, which were validated on the 2D-3D experimental program performed in UPTF, SCTF and CCTF facilities. 3D core simulations using one mesh per assembly may become a standard practice in near future and a local refinement of the highest power assemblies with sub-channel analysis becomes also possible. Looking at much finer multi-dimensional physical processes may provide a better accuracy of predictions but also requires more detailed and precise 3D models with a new specific validation. A detailed PIRT identifies all local flow processes to be considered at such a finer scale. Some of these processes may be neglected depending on the sub-component (core, lower plenum, annular downcomer, upper plenum) and depending on the physical situation encountered in accidental transients. An experimental program using the METERO test facility focuses on SLB, IBLOCA and SBLOCA situations in a PWR core to develop models and to validate them in a separate-effect way. Adiabatic water tests and air-water tests will provide information for the development and validation of turbulent diffusion and dispersion of heat and momentum due to time and space averaging, void dispersion, 3D wall friction and interfacial friction forces in non-isotropic media particularly in presence of non axial flows in a core.

KEYWORDS

Two-phase flow, Pressure Vessel, 3D in porous medium, Validation experiment

1. INTRODUCTION

System thermalhydraulic codes have 3D models in porous medium approach which were initially devoted to the prediction of very large scale 3D effects during LBLOCAS (Large Break Loss of Coolant Accidents) and which were validated on the data of the 2D-3D experimental program performed in UPTF, SCTF and CCTF facilities. 3D modules were used first with rather coarse reactor nodalization including only a few hundreds of meshes in the whole pressure vessel. Today the increased computer power allows 3D simulations with a much finer nodalization for many transients. A core modelling with one mesh per assembly may become a standard practice in near future with the CATHARE code. Also a local refinement of the highest power assemblies with sub-channel analysis modelling is possible. This trend allows to looking at much finer multi-dimensional physical processes and may provide a better accuracy of predictions. New safety requirements may include the fuel relocation in case of a clad ballooning for the LOCA simulations. This is a reason for developing and validating a more detailed and precise core modeling.

Specific requirements are necessary for such finer simulations. First, a PIRT (Phenomena Identification and Ranking Table) exercise identifies dominant phenomena at a smaller scale than for previous nodalizations. Based on porous body 3D equations, one can identify a list of new phenomena (compared to 1D approach) to be modeled and validated on specific separate effect tests. This includes the turbulent diffusion of heat and momentum, the void dispersion, and the heat and momentum dispersion due to space averaging. In addition, 3D wall friction and interfacial friction tensors have to be developed and validated for non-isotropic media like core rod bundles. An order of magnitude analysis allows to neglect some of these processes or simplify some models, depending on the sub-component (core, lower plenum, annular downcomer, upper plenum) and depending on the physical situation encountered in accidental transients.

An experimental program, mainly focused on IBLOCA (Intermediate Break Loss of Coolant Accident) and SBLOCA (Small Break Loss of Coolant Accident) situations in a core of PWRs, is built using the METERO_V test facility to develop models and to validate them in a separate-effect way. It represents at the real scale two half assemblies with 8 x 34 rods and can simulate situations with unbalanced flowrates, fluid temperatures, or void fractions in the two assemblies in order to investigate all radial transfers. Although it is simply using water or air-water in non-heated rods, it can provide useful information for the development and validation of the friction and pressure losses for non-axial flow, the crossflows with radial mixing effects, the diffusion-dispersion of momentum, of energy, or of a passive scalar, the interfacial friction for non-axial flow, and the void dispersion force.

2. SMALL SCALE PROCESSES IN POROUS MEDIUM

Revisiting the PIRT for 3D modelling requires that 3D effects on all models are examined. There may be a geometrical effects on the flow regime and heat transfer regime and on all wall transfers, and interfacial transfers, compared to a 1D flow situation. In addition, in a 3D flow in a porous body, there may also be turbulent diffusion and dispersion of mass, momentum and energy due to time and space averaging. One may also identify specific 3D processes, such as gravity driven natural circulation, mixing layers, jets, wakes, flow curvature,... For each component of the vessel, each phase of each transient of interest, one evaluates the sensitivity of each process on the Figure of Merits (FoMs), the uncertainty on the existing models, the possible effects of specific geometrical details (spacer grids, flow restrictions, nozzles, ...) on the process have to be identified. At last the validation data base is identified with processes which can be validated in a separate-effect way (best case), or validated more globally together with other sensitive processes, or even not validated at all (worst case). This analysis may be first done by expert judgement and then supported by sensitivity calculations. Defaults of the existing models may be identified which require further modelling efforts. Remaining validation needs are also identified.

2.1 Identification of Processes from the Set of Equations

The system of equations used in porous-3D two-fluid model is the basis for identification of all relevant 3D processes. For CATHARE 3, the system of equations reads (see Chandesris et al., [1]):

$$\frac{\partial \phi \alpha_k \rho_k}{\partial t} + \nabla \cdot (\phi \alpha_k \rho_k V_k) = \phi \Gamma_k \quad (1)$$

$$\alpha_k \rho_k \left(\frac{\partial V_k}{\partial t} + V_k \nabla \cdot V_k \right) + \alpha_k \nabla P = (p_i + f_i^{TD}) \nabla \alpha_k + \tau_i + \alpha_k \rho_k g + \tau_{wk} + \frac{1}{\phi} \nabla \cdot (\alpha_k \rho_k \tau_k^{t+d}) \quad (2)$$

$$\frac{\partial \phi \alpha_k \rho_k e_k}{\partial t} + \nabla \cdot (\phi \alpha_k \rho_k h_k V_k) = \phi q_{ki} + S_c q_{wk} + \phi \Gamma_k h_k + \nabla \cdot (\alpha_k q_k^{t+d}) \quad (3)$$

In these equations, $\alpha_k, \rho_k, V_k, e_k, h_k$ are the volume fraction, the density, the velocity, the internal energy and the enthalpy for the phase k , ϕ is the porosity, P the pressure, Γ_k the interfacial mass exchange. p_i and f_i^{TD} are void dispersion terms due to space averaging of interfacial pressure forces, and time averaging of drag and added mass forces. They tend to homogenize void fraction. τ_i is the interfacial friction force, τ_{wk} the wall friction force, q_{ki}, q_{wk} the interfacial and the wall to phase k

heat transfer, S_c the heating surface, τ_k^{t+d} the stress tensor which accounts for turbulent and dispersive effects, and q_k^{t+d} the turbulent and dispersive heat flux.

The momentum and energy dispersive and diffusive terms came out during the double (time and space) averaging process of the local convection terms:

$$\langle \overline{v\bar{v}} \rangle_f = \langle \bar{v} \rangle_f \langle \bar{v} \rangle_f + \langle \overline{v'v'} \rangle_f + \langle \overline{\delta v \delta v} \rangle_f \quad (4)$$

$$\langle \overline{v\bar{h}} \rangle_f = \langle \bar{v} \rangle_f \langle \bar{h} \rangle_f + \langle \overline{v'h'} \rangle_f + \langle \overline{\delta v \delta h} \rangle_f \quad (5)$$

In the previous expressions, \bar{x} is the time average of the quantity x and x' the deviation from this average, and $\langle x \rangle_f$ is the spatial average of the quantity x and δx the deviation from this average. The first rhs (right hand side) terms of equations (4) and (5) are the macroscopic convection of the mean velocity and enthalpy, the second rhs terms are the turbulent diffusion of momentum and energy, and the third rhs terms are momentum and energy dispersion terms.

The void dispersion terms p_i and f_i^{TD} , are related to spatial and temporal fluctuations of pressure and velocity at the interface and represent in dispersed flow (bubbly or droplet flows) the dispersive effect of bubbles or droplets by the turbulence of the continuous phase.

2.2 Core Phenomena

Previous studies provided a rather detailed understanding of dominant phenomena in a PWR core (Valette, 2011, [2], Chandesris et al. 2013 [1], Bestion, 2014 [18], Bestion and Matteo, 2015 [3], Alku, 2017 [4], Bestion et al. 2017 [5]).

Chandesris et al. [1] synthesized the status of modelling and validation of these momentum and energy diffusion and dispersion terms for a PWR core available on option in the CATHARE code. Mainly data in small rod bundles were used and analysed at the sub-channel scale. Today there is no general diffusion-dispersion model validated for every type of meshing and the applicability of current models to large scale nodalizations is not proved. There is a lack of data obtained in large dimension rod bundles with measurement of diffusion and dispersion effects. One can add that diffusion-dispersion of other scalar quantities such as boron concentration also needs validation. Regarding the void dispersion term, Valette [2] proposed some models for core geometry based on PSBT and BFBT benchmark data analysis at the sub-channel scale. However, extension of the models and validation to larger scale modelling is also required.

It was found in a core that dispersive fluxes usually dominate the macroscopic turbulent heat flux by two or three order of magnitude and that turbulent fluxes also dominate molecular fluxes. It is also clear that spacer grids play a dominant role on dispersion effects and that dispersion is highly geometry-dependent. The presence of mixing vanes is playing a dominant role. Although the flow is mainly vertical upwards in a core during LOCAs, rather important radial transfers exist which play a significant role on the Peak Clad Temperature (PCT). Fig. 1 illustrates typical SBLOCA or IBLOCA situation during a core uncovering and LBLOCA during a reflooding. This comes mainly from observations and analysis of previous experimental programs such as PERICLES 2D [6]. In both cases, the two-phase zone below quench fronts or below a swell level is well homogenized by a gravity driven recirculation which may also extend to the zone below the core. In such low velocity flow, the void dispersion force play a minor role in this mixing. This mixing is rather well predicted without specific modelling efforts although the wall friction and interfacial friction for radial flow is not yet correctly addressed. A high uncertainty on these transverse frictions has not a big impact on PCT. In reflooding, the faster quenching in colder zones induces some liquid transfer to hot assembly just above its quench front (by simple gravity effects) which induces a better precooling and increases droplet entrainment in the dry zone of the hot assembly. This accelerates the quenching in hot zone and improves exchanges in dry zone by more steam cooling by droplets. In the swell level zone of a SBLOCA situation, gravity also homogenizes the level. In the dry zone with pure steam, gravity and density differences induce some significant chimney effect which improves the cooling of the hot assembly. It was found (Bestion et al 2015 [1], 2017, [3]) that crossflows may be from hot to cold assembly at lower pressure (e.g. $P < 1$ MPa)

since higher velocity creates more axial friction pressure losses and the crossflow is of diverging type from hot to cold (Fig. 2). The transverse flow pressure losses are not well modelled nor validated and a high uncertainty is still required as long as no Separate Effect Test (SET) validation is available. Momentum and energy diffusion-dispersion may play some role in both situations. However, previous work indicates that they may be of second order compared to crossflows. Recent calculations of core uncovering and reflooding PERICLES tests at the sub-channel scale using the validated diffusion and dispersion models of Chandesris et al. [1] were done by Alku [4] and have shown that the maximum clad temperatures were not very sensitive to any diffusion dispersion term with current models developed in different conditions. Moreover, it was found that all the mixing processes at the periphery of a hot assembly (momentum diffusion-dispersion, heat diffusion-dispersion and crossflows) create mixing layers which enlarge rather slowly so that one may expect that radial gradients within each assembly are never fully eliminated by mixing along the core height and that a high power assembly is probably mainly influenced by its direct neighbours.

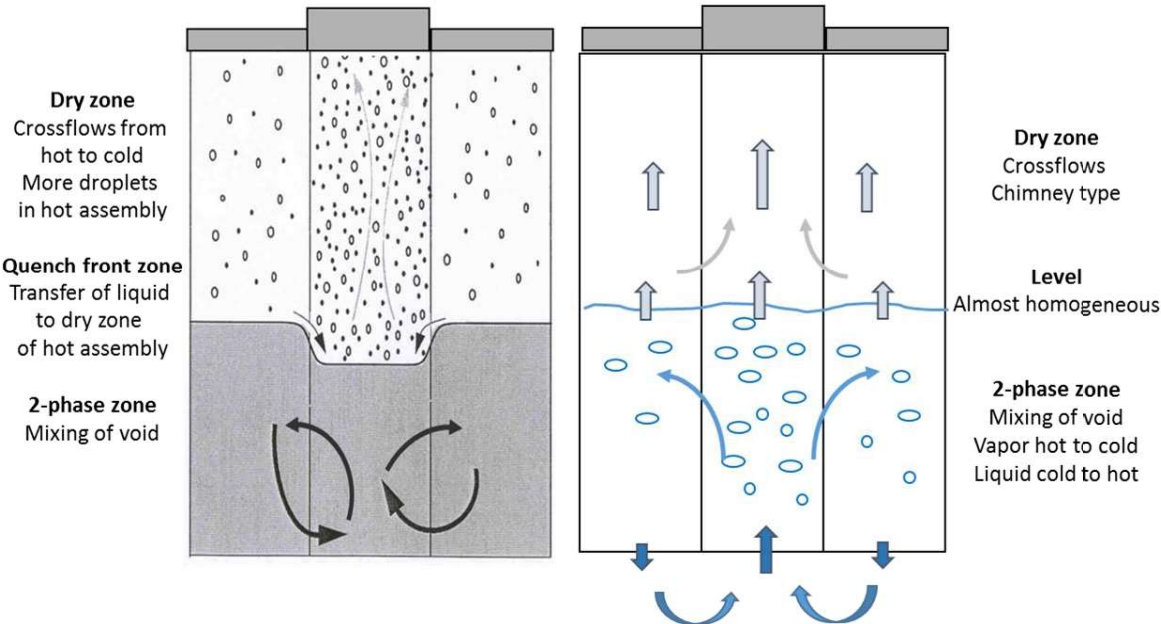


Fig. 1 : Radial transfers due to power profile. A high power assembly with two lower power neighbours. Left: low pressure LBLOCA reflooding; Right: high pressure SBLOCA core uncovering

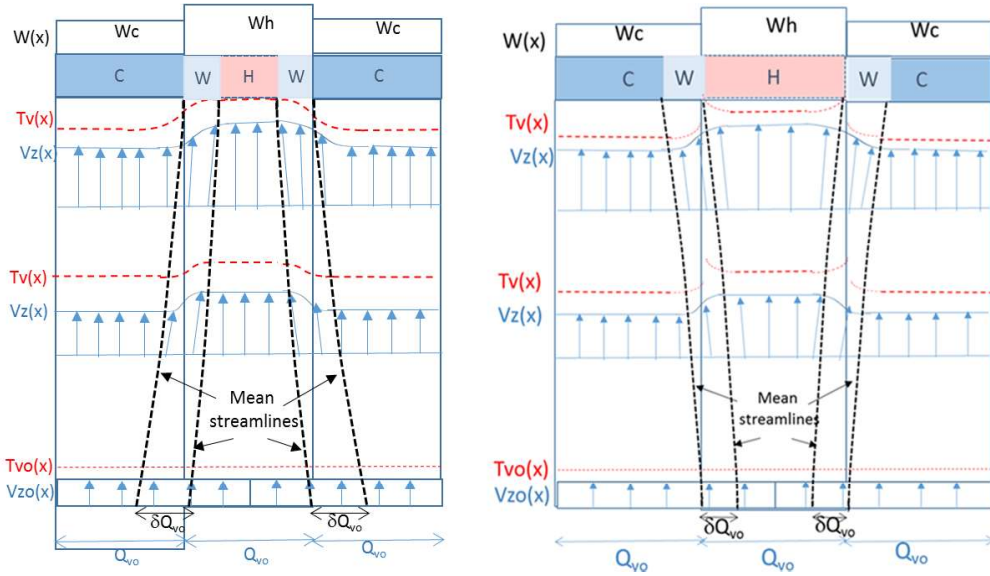


Fig. 2 : Chimney effect on the left and diverging crossflow on the right

One can identify three radial mixing processes between sub-channels or between assemblies:
Radial momentum diffusion-dispersion

- $\tau_{zx}^{d+t} \sim \mu_t \frac{\partial V_z}{\partial x}$ homogenizes radially V_z and creates a radial flow from high V_z to lower V_z

Radial heat diffusion-dispersion

- $q_x^{d+t} \sim \lambda_t \frac{\partial T}{\partial x}$ transfers heat from hot to cold assembly

Crossflow by pressure radial differences

- $\frac{\partial P}{\partial x} = -\frac{K_{effx}}{L_x} \rho \frac{V_x^2}{2}$ transfers fluid from high V_z to lower V_z or from low V_z to high V_z
- transfers energy by convection from hot to cold assembly or from cold to hot assembly.

2.3 Detailed PIRT for 3D Processes in a PWR during a SB-LOCA

The current analysis of processes is summarized in table 1 for SBLOCA. The chimney type crossflow has a favorable effect on PCT since the hottest assembly receives additional coolant flow and a colder coolant from neighbors. Diverging crossflow has a limited unfavorable effect since the hot assembly loses coolant but gives part of its energy to neighbors.

Table 1: PIRT analysis specific to a 3D approach for an uncovered core in a SBLOCA

3D EFFECTS IN AN UNCOVERED PWR CORE OF A SBLOCA				
Process	Sensitivity on FoM (H,M,L)	Model Uncertainty (H, M, L)	Geometry effect	SET or global validation
Flow regime identification	Possibly H	L in axial flow	possible effect of grids	No
Interfacial friction	H	M	probably low	Axial flow:OK Radial flow : no
Wall friction & form loss	M	axial flow: L radial flow: H	Spacer grids	Axial flow:OK Radial flow : no
Void dispersion	L	H	?	No
Interfacial H&M transfers	L (pure vapor in dry zone)			
Wall HT regime identification	H	L		Axial flow:OK
Convection to liquid	L	L	Spacer grids	Axial flow:OK
Nucleate boiling	L	M		Axial flow:OK
CHF (DNB or dry-out)	L to H	M	Spacer grids	OK
Convection to vapor	H	L	Spacer grids	Axial flow:OK
Heat diffusion-dispersion in liquid	L	M	Spacer grids	PSBT
Heat diffusion-dispersion in steam	L or M	M	Spacer grids	No
Specific 3D processes				
• Chimney effect	M	M	Spacer grids	No
• Diverging crossflow	M	M	Spacer grids	PERICLES

H: high; M: medium; L: low

The objective is here to identify processes which are sensitive, not well known (high uncertainty) or which may be sensitive to geometry or to 3D flow conditions (e.g. non axial flow) and which may require additional experimental information.

Many processes are influenced by the geometry of spacer grids.

One may identify a lack of information on the following processes:

- Flow regimes in rod bundles are not well known which induces some significant uncertainty on interfacial friction, swell level, onset of drop entrainment; however visualization in such geometry remains very difficult.
- Wall friction in non axial flow, which influences chimney effect and any crossflow.
- Interfacial friction in non-axial flow
- Diffusion-dispersion of momentum and energy
- Void dispersion

3. NEED OF VALIDATION DATA

3.1 Insight of the current CATHARE validation

The validation of CATHARE against SETs for the radial transfers occurring in a PWR core includes SCFT tests performed in a simulated core consisting of eight bundles arranged in a row. These

experiments are used to analyze the two dimensional thermal–hydraulic behavior and more specifically effects of radial power and temperature distribution [8]. Such radial effects are also validated against PERICLES 2D experiments evoked in section 2.2 and described in detail in the next section, where complementary results are presented.

The different closure laws corresponding to the three diffusion-dispersion terms (momentum and energy dispersive and diffusive terms, void fraction dispersion) were assessed following a step-by-step methodology using various experiments in small rod bundles flows in PWR core geometry. First, the turbulent dispersion of momentum was evaluated using adiabatic single phase (liquid) experiments in rod bundle; then, the turbulent dispersion of liquid energy against experiments with heated rods but without steam production; and finally, the void dispersion against experiments with boiling flow. As mentioned in section 2.2, the 3-D validation program includes two OECD/NRC benchmarks: BFBT and PSBT, with 3-D subchannel calculations using CATHARE 3. The subchannel validation matrix also includes rod bundle tests performed in OMEGA, GRAZIELLA and AGATE facilities [1,2].

3.2 Validation of CATHARE 3D Module Against PERICLES 2D Experiment

3.2.1 Presentation of the PERICLES 2D facility and the BOIL-UP tests

The PERICLES 2D experiment [9,10] was designed to investigate multidimensional effects in a PWR core due to non uniform radial power in both core uncovering (relative to SBLOCAs) and reflooding [5] (relative to LBLOCAs) cases. The experiment consists of a vertical rectangular channel containing three different rod assemblies, denoted here by A, B and C. Each assembly contains $7 \times 17 = 119$ full length heater rods.

The assemblies are heated by two independent electrical power sources, with a possible higher power in the central assembly B (the ‘hot’ assembly) than the two lateral ones A and C (the ‘cold’ assemblies). The heated length of the rods is 3656 mm and the rod diameter is equal to 9.5 mm. This corresponds to the situation shown in Figures 1 and 2.

All rods have the same axial power profile. the higher flux being at mid-elevation. The nominal heat flux densities ϕ in the assemblies A and C are identical and the ratio $\phi(B)/\phi(A,C)$ defines the radial peaking factor. In the test matrix, the nominal values of the heat flux densities ranged from 2.45 W/cm² to 5 W/cm², and the radial peaking factor between 1 and 1.85. The pressure of the system was equal to 3 bar and the water entering the assemblies had 60°C subcooling.

The cladding temperature and the fluid temperature are measured by means of thermocouples. In each assembly, the cladding temperature is measured at 24 different elevations, and the fluid temperature is measured at 6 different elevations.

In the BOIL-UP tests of the PERICLES-2D experiment, a constant subcooled water flowrates and constant power results in a stabilized swell level ZG separating a two-fluid boiling zone from a pure steam flow above ZG. The swell level positions in the different tests ranged from 2.20 m to 3.45 m.

The observed experimental tendencies are the following:

- The axial position of the swell level ZG is quite the same for the three assemblies, even if the radial peaking factor is not equal to 1.
- The void fraction profiles in the three assemblies are close to each other, showing the existence of cross-flows in the wetted zone. The wetted zone is thus characterized by a perfect or quasi-perfect radial mixing.
- The wall to vapor heat transfer in the dry zone is close to the one obtained by assuming a perfect radial mixing in the wetted zone, a uniform steam flux at the swell level and no radial mixing in the dry zone.

3.2.2 Assembly scale validation

The first validation of CATHARE 3D module against the PERICLES-2D tests were made in 1999 [6] using only one mesh per assembly and 11 axial meshes (the minimum required to correctly describe the

axial power profile). Now the computer power allows a finer axial nodalization. So these calculations have been repeated using 14, 28 and 56 axial meshes, corresponding to mesh sizes of 26, 13 and 6.5 cm, respectively.

In the calculations with 28 and 56 axial meshes, the axial pressure drops due to the grids are localized at their exact elevations (instead of an axial spreading in the first validation). The localization of the axial pressure drops has an impact on the radial transfers, as shown in METERO-V pre-calculation part.

The test BO0018 with a radial peaking factor equal to 1.85 and a swell level equal to 2.74 m is presented below. For the three assemblies, the axial profiles of the gas temperatures are shown in Fig. 3 (left) and the axial profiles of the cladding temperatures are shown in Fig. 3 (right). In the two-phase zone, all calculations predict a perfect radial mixing, in agreement with the experimental data.

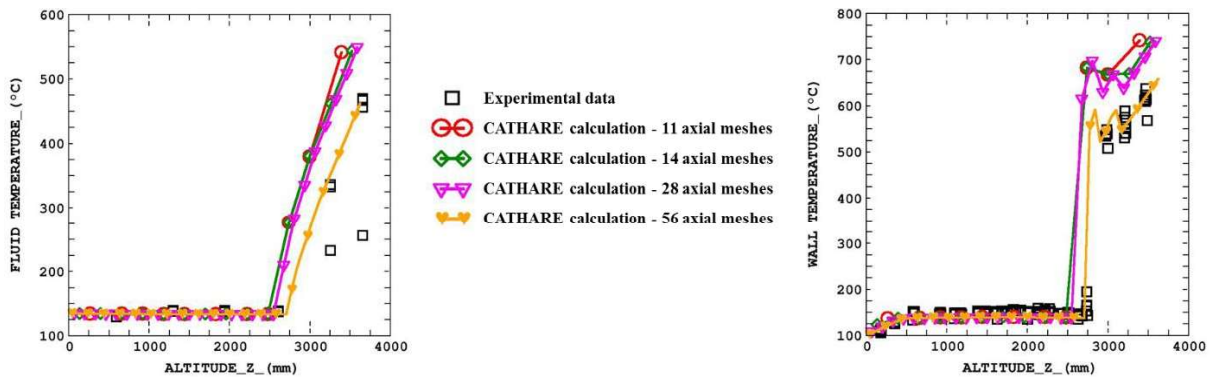


Fig. 3 : Comparison of the vapor temperature (left) and the cladding temperature (right) axial profiles in the hot assembly between CATHARE and the experiment

The finer mesh produces better results than the coarse mesh. since the swell level position is better predicted by the CATHARE calculation (next to its experimental position). So, the start of the temperature increase is localized a little upper in the finer nodalization calculation than in the coarse one; and the predictions are better. The other BOIL-UP tests (not presented in this paper) also validate the use of a finer mesh in the current 3D modelling of the core with CATHARE. A recent modeling of the Pressurized Vessel with CATHARE-3 used 40 axial meshes in the core [12], and the current safety studies use 45 axial meshes in the core [13].

3.2.3 Sub-channel analysis

The PERICLES-2D test BO0018 is here calculated using sub-channel modelling with 56 axial meshes and 51 radial meshes for a better analysis of the radial mixing. A divergent crossflow as in Fig. 2 (right) from hot to cold assemblies is expected due to low pressure conditions. Calculations have been made with and without turbulent diffusion and dispersion effects in order to see the comparative effects of crossflows and diffusion - dispersion effects on the radial temperature profile

The Fig. 4 presents the steam and cladding temperatures at the elevation of 3.4 m:

- The maximum cladding temperature in the hot assembly is at the border of the assembly due to a lower axial velocity, the central temperature being a little lower than the mean value.
- In the cold assemblies, the cladding temperature is quite homogeneous, but tends to be higher for the rod close to the hot assembly in the calculation.

These both observations can be explain by the radial mixing, as shown Fig. 2 (right).

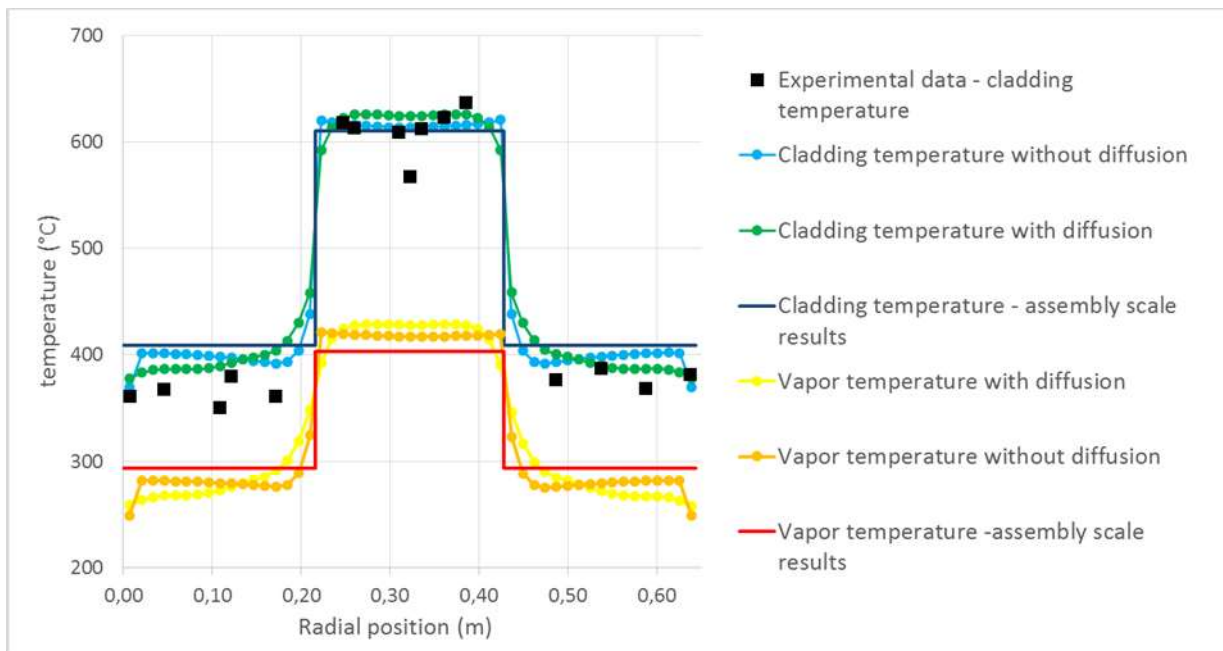


Fig. 4 : Comparison of the cladding temperature radial profiles at the elevation of 3.4 m between CATHARE and the experiment and radial vapor profiles

The turbulent diffusion and dispersion terms leads to larger mixing layers between the assemblies as shown in both steam and clad temperature profiles. Due to the limited number of measurements, no significant comparison of steam profiles can be made and clad temperature profiles can only show a minimum temperature in the center of the hot assembly with maxima at lateral positions, due to divergent crossflows. The curvature of the profile is underestimated by CATHARE, indicating a possible overestimation of the radial pressure losses (modeled with Idel'cik formula in these calculations).

The swell level is not exactly the same in the calculation with 3 and 51 radial meshes explaining the differences on vapor and clad mean values. Moreover, the axial flow rate is very similar between the 3 assemblies in the assembly-scale calculation. In the finer modelization, differences on the gas flow are observed, as shown in Fig. 5. So, the radial mixing in the swell zone is not perfect. This differences have an impact on the gladding temperature. A better knowledge of the 2 phase-flow radial mixing in rod bundle geometry is also needed.

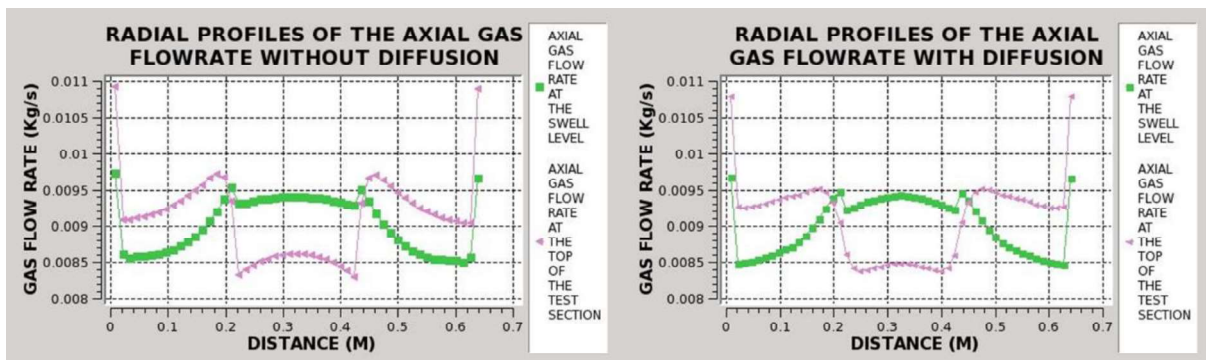


Fig. 5 : Radial profiles of the axial flowrate at the swell level and the top of the test section

To conclude, turbulent diffusion and dispersion terms seems to have a minor effect on the presented PERICLES-2D calculation, but in other situation (with chimney effect or with a higher dry zone), these terms could have a significant impact on the calculation result. So, there clearly a need to increase the capability of CATHARE to models such situation at sub-channel scale which may be used as a reference for the assembly modeling. This is one of the goal of the METERO-V test presented in section 4.

3.3 Other Experiments for Validation of the Radial Transfers in Core

Apart of PERICLES, SCTF or experimental databases in 5x5 to 8x8 rod bundle geometries (PSBT, BFBT, AGATE, GRAZIELLA, ...), other experiments exist for the validation of the radial transfers between assemblies or subchannels. Among them, HERMES experiments [14], performed at CEA-Cadarache on 2 full PWR 17x17 unheated assemblies positioned side by side, comprise runs with a non-uniform inlet flow distribution between the assemblies at high velocity for at least one of the assemblies. The velocities within the subchannels are measured at different elevations of the test section, providing information for the validation of the transverse pressure losses and momentum diffusion-dispersion models. Same type of tests with unbalanced velocities at the inlet of the assemblies are reported by Weiss et al. [15] in a loop built at Westinghouse. The test section consisting of two square rod bundles, each one of 14 x 14 rods. Local velocities and static pressures transverse profiles were measured using Pitot tubes at different levels of the test section. Specific experiments were devoted to the characterization of the transverse pressure loss in a rod bundle, such as EOLE. This CEA/EDF experimental program has been designed to characterize the cross flow through a rod bundle at different inclinations. From the runs, a correlation for the transverse pressure drop coefficient has been proposed. However, because of the limited number of rods (maximum 8 x 8) and the confinement of the flow due to the box of the test section, Bieder [16] demonstrated that the EOLE experiment does not represent correctly the physics of a transverse flow in a fuel assembly of a nuclear reactor core.

Buoyancy-driven flows can be studied using an experiment built at the Pacific Northwest National Laboratory (PNNL) consisting of a 2 x 6 rod bundle, where only the 2 x 3 left rods are heated [17]. Runs are performed at low velocities, involving natural and mixed convections. The power dissymmetry causes transverse velocities due to the buoyancy effect, which can be validated using the velocities and temperatures distributions measured at several locations along the heated length.

The validation database for the 3D effects in a PWR core is more extended than the aforementioned experiments, but the available data, to our knowledge, only cover a part of the domain of interest for the considered phenomena or have to be carefully considered due to some scaling effects such as the insufficient size of the test section. Then a new experimental program is needed to investigate in a separate-effect way all the processes of interest and all the models involved in the 3D effects mentioned in [18] and in section 2.3.

4 METERO-V PROGRAM

The METERO-V (V for vertical) program, supported by CEA, EDF, Framatome and IRSN in the frame of the NEPTUNE project, intends to provide data for the validation of 3D in porous medium models of system codes and sub-channel codes used for core thermalhydraulics modelling. As a side objective, it can also be useful for CFD in open medium validation. As a validation tool for 3D models of system codes, the target is a modelling using a mesh per assembly at least in the region of the highest power assembly. Therefore, all the mixing effects between assemblies which are in the set of equations must be validated.

4.1 Test section and flow conditions

The basic test section is a rod bundle with 8 x 34 unheated rods representing 2 half assemblies (Fig. 6). In a first phase of experiments, the height of the test section will be about 2 m although a full rod bundle length (3.6 to 4 m) is also possible in future studies. The test section intends to be modular in order to adapt to various measurement techniques and to various geometries. The rods and rod arrays will be at scale 1 (rod outer diameter $D = 0.95$ cm, pitch $p=1.26$ cm) but enlarged scale may be also envisaged.

Single-phase water flow or air-water flow conditions at near atmospheric pressure may be investigated. The temperature of the fluid may be ambient (14 to 30°C) with possible heating to create radial temperature difference ΔT at the inlet of the two assemblies up to a maximum of 36°C creating a radial density difference $\Delta \rho$ of about 1%. A separate feeding of each assembly can be implemented to create differences of velocity, temperature, density and tracer concentration between the left and right half-

assemblies.

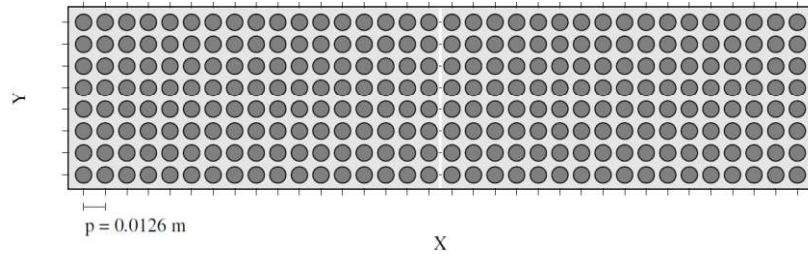


Fig. 6: Radial view of a sketch of METERO-V test section (2 half-assemblies with 8x17 unheated rods each)

4.2 Instrumentation

METERO-V will use the following instrumentation:

- PIV (Particle Image Velocimetry): 2 components of the velocity (1 phase tests)
- LIF (Laser-induced Fluorescence): concentration , temperature (1 phase tests)
- X-ray tomography: linear void fraction (2-phase tests)
- Thermocouples: temperature (1 phase tests)
- Pressure: Pressure and pressure differences (1 phase and 2-phase tests)

PIV will be able to measure profiles of axial and radial components [$V_x(x,z)$, $V_z(x,z)$] of the velocity in the domain of sub-channels visible through rod gaps. Measurements of the radial component may not be accurate if it is much smaller than the axial component.

LIF will use the variation of the luminescence of injected tracers with pH or with temperature. It will be able to measure passive tracer radial concentration profiles $c(x,z)$ at various elevations and temperature radial profiles $T_f(x,z)$ at various elevations.

Temperatures may also be measured by wall thermocouples to give $T(x,z)$. The possibility to use thermocouples at centers of sub-channels will be studied.

X-ray tomography will be used in two-phase air-water tests to measure linearly averaged void fraction (along Y direction) to obtain $\langle \alpha \rangle_y(x,z)$. In order to measure not only between rods but also through rods, Plexiglas rods (or stretch of rods in Plexiglas) will be used.

Pressure P and pressure differences ΔP will be measured at several positions on lateral face (y,z) and front face (x,z) of the test section to measure all kinds of pressure losses. Preliminary simulations using sub-channel modelling will be made to optimize the positions of the pressure taps in order to get the most precise information on the axial and radial pressure losses coefficients for bare rod bundle, and for spacer grids.

4.3 The METERO-V Test matrix

Various test series are planned to address the respective processes of interest. They are summarized in table 2. Such tests do not represent SBLOCA situations but include all processes of a SBLOCA situation. When sub-channel models and 1 mesh/per assembly models will be validated on such tests, more complex and representative SBLOCA situations may be simulated at sub-channel scale to obtain reference results for the 1 mesh/per assembly models. At last a global validation on existing large scale tests may be done using PERICLES data and some IET LOCA tests with radial power profiles such as some ROSA IV-LSTF tests.

Table 2: Test series in METERO test facility

Process	Term of equation	Test series	Test conditions

Wall friction	$\overline{\tau_{wk}}$	<ul style="list-style-type: none"> • P losses in axial flow • P losses in non-axial flow 	<ul style="list-style-type: none"> • Equal BC • UV
Momentum diffusion-dispersion	v_{tk}^ϕ	<ul style="list-style-type: none"> • Pressure losses with transverse flow 	<ul style="list-style-type: none"> • UV-UT-equal $\frac{\partial P}{\partial z}$ • With & without spacers
Scalar turbulent diffusion	d_{tk}^ϕ	<ul style="list-style-type: none"> • Mixing of a passive scalar in 1-phase flow 	<ul style="list-style-type: none"> • EV-US No spacers
Scalar dispersion	$\underline{\underline{D}}_{dk}^\phi$	<ul style="list-style-type: none"> • Mixing of a passive scalar in 1-phase flow 	<ul style="list-style-type: none"> • EV-US
Energy turbulent diffusion	α_{tk}^ϕ	<ul style="list-style-type: none"> • Energy mixing in 1-phase flow 	<ul style="list-style-type: none"> • UT No spacers
Energy dispersive tensor	$\underline{\underline{D}}_{dk}^\phi$	<ul style="list-style-type: none"> • Energy mixing in 1-phase flow 	<ul style="list-style-type: none"> • UT
Two-phase wall friction And two-phase interfacial friction	$\overline{\tau_{wk}}$ $\overline{\tau}_i$	<ul style="list-style-type: none"> • P losses and wall & interfacial friction in axial flow • P losses and wall & interfacial friction with transverse flows • P losses and wall & interfacial friction with buoyancy driven crossflows 	<ul style="list-style-type: none"> • EV-EX • UV-EX • UV-UX
Void dispersion	f_i^{TD}	<ul style="list-style-type: none"> • Void dispersion tests 	<ul style="list-style-type: none"> • UV-UX- equal $\frac{\partial P}{\partial z}$

UV: unequal velocity; EV equal velocity; ES equal scalar (tracer concentration); US unequal scalar concentration; UT: unequal temperature; UX: unequal quality; equal $\frac{\partial P}{\partial z}$ means that velocity differences and temperature or quality difference are such that the axial P gradient are equal to avoid crossflows and to measure scalar or temperature or void diffusion-dispersion

4.4 Example of METERO-V Pre-Calculations

In METERO-V, the radial temperature mixing may be studied using a homogeneous velocity and an unbalanced temperature measurable by LIF. Particles are injected whose luminescence is sensitive to temperature. Crossflow are buoyancy driven when gravitational axial pressure gradient dominates the friction axial pressure losses. The difference of temperature induces density differences which create different axial pressure gradients in the two assemblies. This creates radial pressure differences and crossflows from cold assembly to hot assembly. As soon as crossflows are significant, they may overpass diffusive radial mixing.

The flow configurations of Fig. 7 (a) are used with low homogeneous inlet velocity and temperature differences; here also the crossflows in bare rod bundle and with spacer grids may be investigated separately.

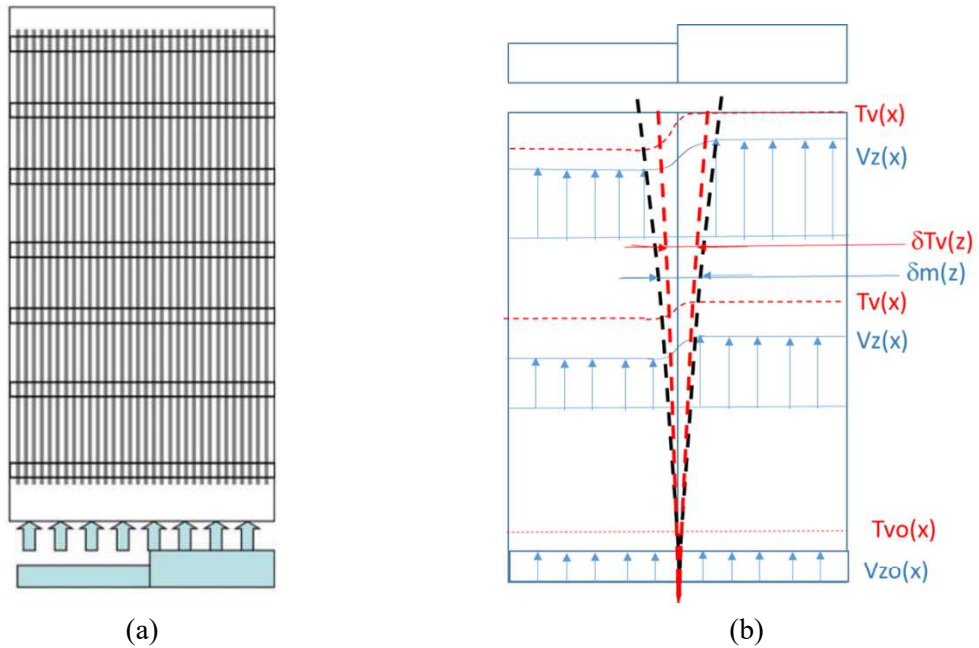


Fig. 7: (a): Temperature mixing test conditions with buoyancy driven crossflows. (b): Axial evolution of the temperature and velocity mixing layers, in case of power difference between the assemblies.

Some simulations using CATHARE 3 were performed to verify if the identified 3D phenomena might be reproduced in the METERO-V conditions. These simulations may also help building the test matrix and determining the range of the measured quantities (temperature, velocities, concentration,...).

Among these simulations, runs with a temperature increment at the inlet of the test section inducing buoyancy driven crossflows were carried out, at the assembly scale and at the subchannel scale. At the last scale, diffusion dispersion terms of the momentum and energy equations were taken into account. Indeed, single-phase PSBT tests using CATHARE 3 with a radial map of the rod power showed that the current model for the diffusion/dispersion energy term improves significantly the prediction of the liquid temperature radial distribution for such a small rod bundle [2], and, as it has been showed in section 3.2.3, has also an impact on the vapor temperature distribution for the PERICLES 2D BOIL-UP tests.

For a uniform velocity $V = 0.10$ m/s and for a liquid temperature increment ΔT between the two assemblies equal to 7°C ($T_{\text{left}} = 20^\circ\text{C}$, $T_{\text{right}} = 27^\circ\text{C}$) at the inlet of the test section, Fig. 8 shows the 2D map in (X,Z) plane of the liquid temperature at the Y centerline of the test section, obtained by CATHARE 3 with a subchannel meshing, and with the current models for diffusion and dispersion terms. This result well illustrates the expected results concerning the mixing layer thickness δT for the temperature where two assemblies have a temperature difference or are unequally heated (see Fig. 7(b)): a mixing layer thickness limited to a few subchannels at the bottom of the assemblies, becoming bigger at the top. Calculations with and without diffusion-dispersion terms of momentum and energy allow to identify the part of the crossflows and the diffusion-dispersion terms on the temperature distribution. Data provided by the future METERO-V runs will validate and/or recalibrate the current diffusion-dispersion terms already validated against experiments at higher Reynolds numbers or at high-pressure conditions [1,2].

Apart of the characterization of the singular pressure loss due to the spacer grids, METERO-V will allow also to quantify the impact of these grids, especially the mixing vane, on the crossflows. Simulations at the assembly or at the subchannel scale showed a significant impact of the grids for the crossflows. With the same inlet temperatures (20°C and 27°C) and velocity (0.10 m/s) as the previous runs, a simulation was performed assuming a first grid located 25 cm downstream the entrance of the test section, and grids

located at each 50 cm along the test section, and compared with a simulation where these grids are “spread” on each vector node along the test section, with the same global singular pressure drop coefficient. On the Fig. 9 (left), the assembly-scale simulations show the impact of the grids on the radial velocity V_x along the Z-direction: the overall behavior is the same with both simulations, with and without grid location, where a chimney effect is predicted, but locally the chimney effect is reduced or even inverted (i.e. a divergent effect is simulated) just upstream the grids. The same behavior is found with simulations performed at the subchannel scale (Fig. 9 (right)). However, we have in mind that such effects will be difficult to measure using PIV technique in this configuration, or with a large uncertainty, because of the very low radial velocities (< 1 cm/s according the presented simulation) regarding the axial velocities (~ 10 cm/s). Tests with a lower axial velocity and with a higher temperature difference between the assemblies will be more favorable to quantify the impact of the spacer grids on the crossflows.

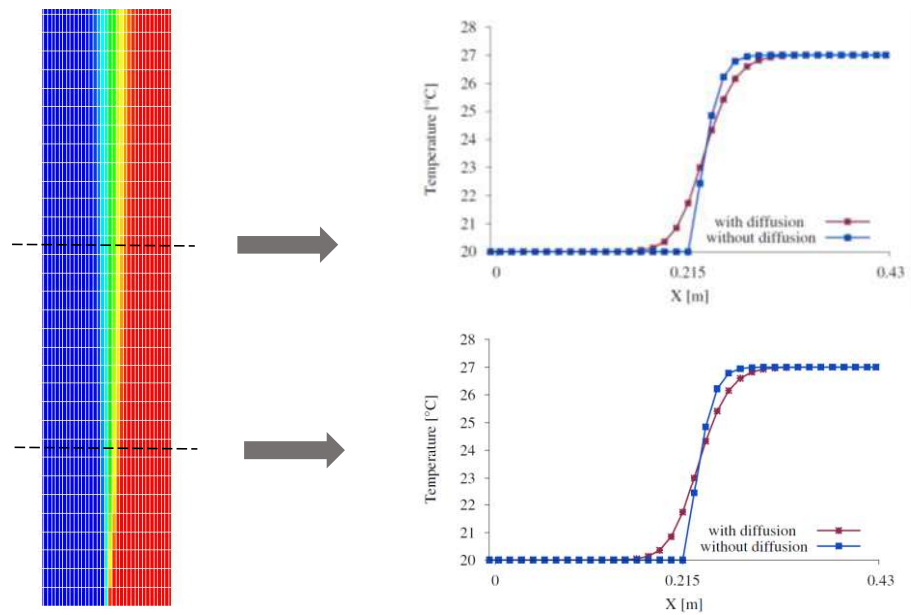


Fig. 8. METERO-V pre-calculations: lower part view of the 2D map of the calculated liquid temperature with inlet temperature increment (left), and temperature profiles along X axis at $Z=0.53$ m and $Z=1.22$ m of the temperature with and without diffusion/dispersion terms (right).

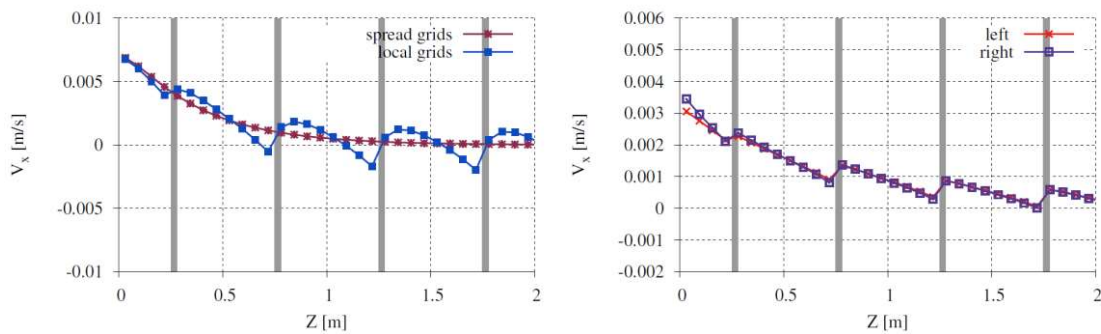


Fig. 9: METERO-V pre-calculations: (left) calculated radial velocity V_x (left assembly to right) along the Z-direction at assembly scale, with and without grids location, and (right) calculated radial velocity V_x at the left and right side of the central subchannel, with grids location. The locations of the grids are marked by thick vertical grey lines.

5 CONCLUSIONS

A PIRT analysis refined at the local level identified dominant processes controlling local 3D effects in a PWR core. The diffusion and dispersion terms in momentum and energy equations and the void dispersion force require some attention. The 3D formulation of wall friction and interfacial friction must be considered as well as the 3D formulation of wall and interfacial heat and mass transfers. Existing experimental data are not sufficient and new needs led to the definition of the METERO-V program.

This experimental program with a test section with 8 x 34 unheated rods representing 2 half assemblies is on ongoing. A matrix of runs, with different configurations with unbalanced temperature, velocity or tracer concentration between the assemblies, is being developed with the help of pre-calculations. Simulations of temperature increment at the inlet of the test section inducing buoyancy driven crossflows were carried out, allowing to show the impact of the diffusion-dispersion term on the temperature distribution. The role of the spacer grids on the crossflows has also been highlighted. Data provided by METERO-V will be used to progress in the validation of the models involved in the 3D simulation of the core during PWR LOCA with a system code, but also could be used at smaller scales.

ACKNOWLEDGMENTS

This work is performed as a joint effort of Commissariat à l’Energie Atomique (CEA), Electricité de FRANCE (EDF), FRAMATOME, and IRSN in the frame of the CATHARE code development.

REFERENCES

1. M. Chandesris, M. Mazoyer, G. Serre and M. Valette, “Rod bundle thermalhydraulics mixing phenomena: 3D analysis with CATHARE 3 of various experiments”, *Proceedings of 15th International Topical Meeting on Nuclear Reactor Thermal Hydraulics (NURETH-15)*, Pisa, Italy (2013).
2. M. Valette, “Analysis of Subchannel and Rod Bundle PSBT Experiments with CATHARE 3”, *Science and Technology of Nuclear Installations*, Article ID 123426 (2012).
3. D. Bestion and L. Matteo, “Scaling considerations about LWR core thermalhydraulics”, *Proceedings of 16th International Topical Meeting on Nuclear Reactor Thermal Hydraulics (NURETH-16)*, Chicago, IL, USA, August 30-September 4, 2015.
4. T. Alku, “Modelling of turbulent effects in LOCA conditions with CATHARE-3”, *Nuclear Engineering and Design*, **321** pp. 258–265, (2017).
5. D. Bestion, P. Fillion, P. Gaillard, M. Valette, “3D core thermalhydraulic phenomena in PWR SB-LOCAs and IB-LOCAs”, *Proceedings of 17th International Topical Meeting on Nuclear Reactor Thermal hydraulics (NURETH-17)*, Xian, China, Sept 3-8, (2017).
6. C. Morel and D. Bestion, “Validation of the CATHARE code against PERICLES 2D BOIL-UP Tests”, *Proceedings of 9th International Topical Meeting on Nuclear Reactor Thermal hydraulics (NURETH-9)*, San Francisco, California, USA, October 3-8, (1999).
7. D. Bestion, “Specific requirements for BEPU methods using System Thermalhydraulic codes with 3D-Pressure Vessel Modelling”, *Proceedings of ANS Best Estimate Plus Uncertainty International Conference (BEPU 2018)*, Real Collegio, Lucca, Italy, May 13-19 (2018).
8. I. Dor and P. Germain, “Core radial profile effect during reflooding, validation of CATHARE 2 3D module using SCTF tests”, *Proceedings of 14th International Topical Meeting on Nuclear Reactor Thermal hydraulics (NURETH-14)*, Toronto, Canada (2011).
9. H.J. Reinhardt, “A study of 2-Dimensional Effects in the Core of a PWR during the Reflooding Phase of a LOCA. Analysis of Data of PERICLES Experiments with the COBRA-NC code”, *Final Report, Commission of the European Communities, Nuclear Science and Technology, Shared Cost Action, Reactor Safety Programme 1985-1987*, September (1989).

10. R. Deruaz, P. Clement, J.M. Veteau, "2D effects in the core during the reflooding phase of a LOCA, Safety of Thermal Water Reactors", *Proceedings of a Seminar on the Results of the European Communities' Indirect Action Research Programme on Safety of Thermal Water Reactors*, Brussels, Belgium, October 1-3, (1984), Published in 1985 by Graham & Trotman Limited.
11. C. Morel and P. Boudier, "Validation of the CATHARE code against PERICLES 2D REFLOODING Tests", *Proceedings of 9th International Topical Meeting on Nuclear Reactor Thermal hydraulics (NURETH-9)*, San Francisco, California, USA, October 3-8, (1999).
12. R. Prea, V. Figerou, A. Mekkas and A. Ruby, "CATHARE-3: a first computation of a 3-inch break loss-of-coolant accident using both cartesian and cylindrical 3D meshes modelling of a PWR vessel", *Proceedings of 17th International Topical Meeting on Nuclear Reactor Thermal hydraulics (NURETH-17)*, Xian, China, Sept 3-8, (2017).
13. H. Geiser, J.-L. Vacher and P. R. Rubiolo, "The Use of Integral Effects Tests for the Justification of New Evaluation Models Based on the BEPU Approach", *Proceedings of 17th International Topical Meeting on Nuclear Reactor Thermal hydraulics (NURETH-17)*, Xian, China, Sept 3-8, (2017).
14. A. Bergeron, D. Caruge and P. Clément, "Assessment of the 3-D Thermal-Hydraulic Nuclear Core Computer Code FLICA-IV on Rod Bundle Experiments", *Nuclear Technology*, **134**(1), pp. 71-83 (2001).
15. E. Weiss, R.A. Markley and A. Battacharyya, "Open duct cooling-concept for the radial blanket region of a fast breeder reactor", *Nuclear Engineering and Design*, **16**, pp. 375-386 (1971).
16. U. Bieder, "CFD analysis of non-axial flow in fuel assemblies", *Proceedings of 16th International Topical Meeting on Nuclear Reactor Thermal Hydraulics (NURETH-16)*, Chicago, IL, USA, August 30-September 4 (2015).
17. J.M. Bates and E.U. Khan, "Investigation of Combined Free and Forced Convection in a 2x6 Rod Bundle during Controlled Flow Transients", Technical report PNL-3135 <https://www.osti.gov/biblio/7042813> (1980).
18. D. Bestion, "Validation data needs for CFD simulation of two-phase flow in a LWR core", *CFD4NRS-5*, Zurich, Switzerland (2014).